OPEN ACCESS
[DOI]10.12016/j.issn.2096-1456.202660064

·基础研究·

乳酸介导的组蛋白乳酸化对骨髓间充质干细胞衰老及成骨分化的影响

郭徐斐，　聂永帅，　杨国斌
武汉大学口腔医院综合科，武汉大学口腔医学院，口颌系统重建与再生全国重点实验室，口腔生物医学教育部重点实验室，口腔医学湖北省重点实验室，湖北 武汉（430079）

【摘要】　目的　探究乳酸生成及组蛋白乳酸化在小鼠骨髓间充质干细胞（BMSCs）衰老过程中的表达变化，以及乳酸代谢对衰老BMSCs成骨分化的影响，为衰老相关骨质疏松及骨修复障碍的代谢调控干预提供实验基础。**方法**　获得单位实验动物伦理委员会审批，采用全骨髓贴壁法提取小鼠BMSCs，经流式细胞术鉴定表面标志物（CD29、CD90、CD11b、CD45）。建立不同浓度依托泊苷（0、5、10、15、20 μmol/L）诱导BMSCs衰老的细胞模型，通过qRT-PCR和Western blot检测衰老相关指标（p53、p21、p16）基因和蛋白的表达水平，结合CCK-8和SA-β-gal实验确定最适诱导浓度。将BMSCs分为对照组和依托泊苷诱导衰老组，检测乳酸生成水平和组蛋白乳酸化相关酶（Ldha、Ep300、Sirt2）的表达；采用Western blot检测泛赖氨酸乳酸化（Pan-Kla）及组蛋白H3第18位赖氨酸乳酸化（H3K18la）的变化。抑制乳酸生成实验中，将BMSCs分为对照组、衰老组（10 μmol/L依托泊苷处理）、衰老+GNE-140组（10 μmol/L依托泊苷+1 μmol/L GNE-140处理），通过qRT-PCR、Western blot及SA-β-gal染色评估抑制乳酸生成对细胞衰老表型的影响。成骨分化实验中，设置对照组、衰老组（10 μmol/L依托泊苷处理）、衰老+5 mmol/L乳酸钠组、衰老+10 mmol/L乳酸钠组，采用Western blot检测Pan-Kla和H3K18la的水平，qRT-PCR检测Runt相关转录因子2（Runx2）、成骨特异性转录因子Sp7（Sp7）、碱性磷酸酶（Alpl）mRNA表达；Western blot检测Ⅰ型胶原（COL1）、RUNX2、成骨特异性转录因子（OSX）、骨钙素（OCN）蛋白表达；茜素红染色观察BMSCs形成矿化结节的情况。**结果**　流式细胞术显示，BMSCs高度表达CD29（97.3%）和CD90（95.7%）。依托泊苷以10 μmol/L为最适浓度，通过激活p53-p21通路诱导衰老。与对照组相比，衰老BMSCs中乳酸生成减少，Ldha、Ep300 mRNA表达下降（$P < 0.001$），Sirt2 mRNA上调（$P < 0.01$），Pan-Kla和H3K18la修饰水平下调（$P < 0.001$）。使用GNE-140抑制乳酸生成后，p53、p21表达及SA-β-gal阳性细胞比例进一步升高（$P < 0.01$）。成骨分化实验中，衰老BMSCs的Runx2、Sp7、Alpl mRNA与COL1、RUNX2、OSX、OCN蛋白表达水平及矿化结节形成能力均下降（$P < 0.05$）；外源性补充5 mmol/L和10 mmol/L乳酸钠可增加泛乳酸化和组蛋白乳酸化水平，并改善衰老BMSCs的成骨分化能力，促进矿化结节形成。**结论**　BMSCs衰老伴随着乳酸生成减少和组蛋白乳酸化修饰水平降低；外源性补充乳酸钠可改善衰老BMSCs的成骨分化障碍。

【关键词】　乳酸；　组蛋白乳酸化；　骨髓间充质干细胞；　细胞衰老；　成骨分化；　骨质疏松；　代谢干预；　茜素红；　SA-β-gal；　组织再生
【中图分类号】　R78　**【文献标志码】**　A　**【文章编号】**　2096-1456（2026）08-0744-13
【引用著录格式】　郭徐斐，聂永帅，杨国斌. 乳酸介导的组蛋白乳酸化对骨髓间充质干细胞衰老及成骨分化的影响[J]. 口腔疾病防治, 2026, 34(8): 744-756. doi:10.12016/j.issn.2096-1456.202660064.

微信公众号

Effect of lactate-mediated histone lactylation on senescence and osteogenic differentiation of bone marrow mesenchymal stem cells　GUO Xufei, NIE Yongshuai, YANG Guobin.　Department of General Dentistry, School and Hospital of Stomatology, Wuhan University, State Key Laboratory of Oral & Maxillofacial Reconstruction and Regeneration, Key Laboratory of Oral Biomedicine Ministry of Education, Hubei Key Laboratory of Stomatology, Wuhan 430079,

【收稿日期】2026-02-09；　**【修回日期】**2026-04-16
【基金项目】国家自然科学基金项目（82270947）
【作者简介】郭徐斐，硕士研究生在读，Email: 2636219750@qq.com
【通信作者】杨国斌，教授，博士，Email: guobin.yang@whu.edu.cn

China.
Corresponding author: YANG Guobin, Email: guobin.yang@whu.edu.cn

【Abstract】 **Objective** To investigate changes in lactate and histone lactylation during senescence of mouse bone marrow mesenchymal stem cells (BMSCs), to clarify the effects of regulating lactate metabolism on the osteogenic differentiation of senescent BMSCs, and to provide theoretical evidence and an experimental basis for metabolic regulatory interventions in aging-related osteoporosis and impaired bone repair. **Methods** Approval was obtained from the Institutional Laboratory Animal Ethics Committee. BMSCs were isolated using the whole bone marrow adherence method and surface markers (CD29, CD90, CD11b and CD45) and identified by flow cytometry. A cellular model of BMSCs senescence was established using different concentrations of etoposide (0, 5, 10, 15, and 20 μmol/L). The gene and protein expression levels of senescence-related markers, namely, p53, p21, and p16, were detected by quantitative reverse transcription polymerase chain reaction (qRT-PCR) and Western blot analysis, and the optimal induction concentration was determined using CCK-8 and SA-β-gal assays. BMSCs were divided into a control group and an etoposide-induced senescence group to examine lactate production and the expression of histone lactylation-related enzymes, including Ldha, Ep300, and Sirt2. Western blot analysis was used to analyze pan-lysine lactylation（Pan-Kla）and histone H3 lysine 18 lactylation（H3K18la). During the lactate production inhibition experiments, BMSCs were divided into three groups: control, senescence group (treated with 10 μmol/L etoposide), and senescence + GNE-140 group (treated with 10 μmol/L etoposide and 1 μmol/L GNE-140). qRT-PCR, Western blot, and SA-β-gal staining were performed to assess the effects of lactate production inhibition on cellular senescence phenotypes. During osteogenic differentiation, BMSCs were assigned to a control group, senescence group (treated with 10 μmol/L etoposide), senescence + 5 mmol/L sodium lactate group, and senescence + 10 mmol/L sodium lactate group. The levels of Pan-Kla and H3K18la were detected by Western blot. The mRNA expressions of runt-related transcription factor 2 (Runx2), transcription factor Sp7 (Sp7) and alkaline phosphatase (Alpl) were detected by qRT-PCR. The protein expressions of collagen type I (COL1), RUNX2, osterix (OSX) and osteocalcin (OCN) were detected by Western blot, and mineralized nodule formation was observed by Alizarin Red S staining. **Results** Flow cytometry analysis indicated that the isolated BMSCs highly expressed CD29 (97.3%) and CD90 (95.7%). Etoposide induced BMSC senescence by activating the p53 – p21 signaling pathway, with an optimal concentration of 10 μmol/L. Compared with the control group, BMSCs exhibited decreased lactate production, reduced mRNA expression of Ldha and Ep300 ($P < 0.001$), upregulated Sirt2 expression ($P < 0.01$), and diminished levels of Pan-Kla and H3K18la modification ($P < 0.001$). Further inhibition of lactate production with GNE 140 further increased the expression levels of p53 and p21 and the percentage of SA β gal positive cells ($P < 0.01$). In osteogenic differentiation experiments, the expression levels of Runx2, Sp7, Alpl mRNA and COL1, RUNX2, OSX, OCN proteins, as well as the mineralized nodule formation ability of senescent BMSCs, were decreased ($P < 0.05$); exogenous supplementation with 5 mmol/L and 10 mmol/L sodium lactate can increase the levels of panolactic lactation and histone lactation, and improved the osteogenic differentiation capacity and mineralized nodule formation of senescent BMSCs. **Conclusion** BMSC senescence is associated with reduced lactate production and decreased histone lactylation levels. Exogenous supplementation with sodium lactate partially rescues osteogenic differentiation impairment in senescent BMSCs.

【Key words】 lactate; histone lactylation; bone marrow mesenchymal stem cells; cell senescence; osteogenic differentiation; osteoporosis; metabolic intervention; Alizarin Red S; SA-β-gal; tissue regeneration
J Prev Treat Stomatol Dis, 2026, 34(8): 744-756.

骨髓间充质干细胞(bone marrow mesenchymal stem cells,BMSCs)是在骨稳态和骨再生中发挥关键作用的细胞[1]。然而,衰老相关的代谢紊乱和表观遗传异常显著限制了BMSCs的再生潜能[2-3]。并且BMSCs的衰老被认为是骨量丢失和退行性骨疾病发生发展的关键细胞学基础[4]。因此,深入阐明调控BMSCs衰老和分化的分子机制,对于提升其在骨再生与骨衰老干预中的应用价值具有重要意义。

近年来研究表明,细胞代谢重编程及表观遗传调控在干细胞衰老和分化命运决定中发挥重要作用[5-6],乳酸不仅是糖酵解代谢的重要产物,还可作为信号分子参与细胞功能调控。2019年,研究人员首次发现乳酸能够通过修饰组蛋白赖氨酸残基形成组蛋白乳酸化,从而将细胞代谢状态与基

因转录调控相联系。后续研究表明，组蛋白乳酸化参与炎症反应、细胞分化及衰老过程[7-9]。然而，目前关于组蛋白乳酸化在BMSCs衰老过程中的动态变化及其对成骨分化调控作用仍缺乏系统研究。笔者推测，BMSCs衰老过程乳酸生成水平发生变化，进而改变组蛋白乳酸化水平，影响相关基因表达，最终参与衰老BMSCs成骨分化能力的调控。

基于此，本研究以小鼠BMSCs为研究对象，构建依托泊苷诱导的细胞衰老模型，结合乳酸代谢水平检测、组蛋白乳酸化修饰分析及成骨分化功能评价，系统探讨BMSCs衰老过程中乳酸代谢及组蛋白乳酸化的变化特征，并阐明其对衰老BMSCs成骨分化能力的调控作用，为揭示代谢-表观遗传互作在骨组织衰老中的作用提供新的理论依据，并为靶向调控干细胞衰老、改善骨再生能力及退行性骨疾病的干预策略提供思路。

1　材料和方法

1.1　主要试剂和仪器

α-最小必需培养基（alpha minimal essential medium，α-MEM）（SH30625.01，Hyclone，美国）；胎牛血清（fetal bovine serum，FBS）（SH30406.05，Hyclone，美国）；青霉素-链霉素溶液（SV30010，Hyclone，美国）；胰酶（25200072，Gibco，美国）；依托泊苷（HY-13629，MCE，美国）；L-乳酸钠（71718，Sigma-Aldrich，美国）；乳酸脱氢酶抑制剂GNE-140（HY-100742，MCE，美国）；β-甘油磷酸钠（G9422，Sigma-Aldrich，美国）；维生素C（A4544，Sigma-Aldrich，美国）；地塞米松（D4902，Sigma-Aldrich，美国）；FITC标记抗小鼠CD29抗体（102205，Biolegend，美国）；FITC标记抗小鼠CD90.2抗体（105305，Biolegend，美国）；FITC标记抗小鼠CD11b抗体（101205，Biolegend，美国）；FITC标记抗小鼠CD45抗体（157607，Biolegend，美国）；β-actin鼠单克隆抗体（1∶10 000，66009-1-Ig，武汉三鹰，中国）；H3兔多克隆抗体（1∶10 000，17168-1-AP，武汉三鹰，中国）；肿瘤蛋白P53（tumor protein p53，p53）兔多克隆抗体（1∶10 000，10442-1-AP，三鹰，中国）；细胞周期蛋白依赖性激酶抑制剂2A（cyclin-dependent kinase inhibitor 2A，p16）兔多克隆抗体（1∶1 000，HA723746，华安，中国）；细胞周期蛋白依赖性激酶抑制剂1A（cyclin-dependent kinase inhibitor 1A，p21）兔多克隆抗体（1∶1 000，HA722065，华安，中国）；泛赖氨酸乳酸化（pan-lysine lactylation，Pan-Kla）兔单克隆抗体（1∶1 000，PTM-1401RM，景杰，中国）；组蛋白H3第18位赖氨酸乳酸化（histone H3 lysine 18 lactylation，H3K18la）兔单克隆抗体（1∶1 000，PTM-1427RM，景杰，中国）；Runt相关转录因子2（runt-related transcription factor 2，Runx2）兔单克隆抗体（1∶1 000，CY5864，Abways，中国）；成骨特异性转录因子Sp7（transcription factor Sp7，Sp7/Osterix，Osx）兔多克隆抗体（1∶1 000，ab22552，Abcam，美国）；Ⅰ型胶原（collagen type Ⅰ，Col1）兔多克隆抗体（1∶1 000，66761-1-Ig，三鹰，中国）；骨钙素（osteocalcin，Ocn）兔多克隆抗体（1∶1 000，A20800，Abclonal，中国）；二抗山羊抗兔抗体（1∶5 000，ANT020，安特捷，中国）；二抗山羊抗鼠抗体（1∶5 000，ANT019，安特捷，中国）；Gapdh、p53、p21、p16、Runx2、Sp7、碱性磷酸酶（alkaline phosphatase，Alpl）、乳酸脱氢酶A（lactate dehydrogenase A，Ldha）、E1A结合蛋白p300（E1A binding protein p300，Ep300）、沉默信息调节因子2（sirtuin 2，Sirt2）引物（擎科，中国）；细胞衰老β-半乳糖苷酶染色试剂盒（C0602，碧云天，中国）；L-乳酸检测试剂盒（A019-2-1，南京建成，中国）；BCA蛋白浓度测定试剂盒（P0010，碧云天，中国）；增强化学发光（enhanced chemiluminescence，ECL）试剂盒（K-12045-D50，Advansta，美国）；茜素红染液（ALIR-10001，赛业，中国）；HiScript Ⅱ Q RT SuperMix for qPCR（R223-01，诺唯赞，中国）；ChamQ Blue Universal SYBR qPCR Master Mix（Q312-02，诺唯赞，中国）。

倒置相差显微镜（CKX53，Olympus，日本）；流式细胞仪（CytoFLEX LX，Beckman Coulter，美国）；实时荧光定量PCR仪（LightCycler 96，Roche，瑞士）；酶标仪（Multiskan FC，Thermo Scientific，美国）；电泳仪（PowerPac Basic，BIO-RAD，美国）；转膜仪（Trans-Blot Turbo，BIO-RAD，美国）；化学发光凝胶成像系统（ChemiDoc XRS+，BIO-RAD，美国）。

1.2　方法

1.2.1　BMSCs的分离、培养及鉴定　6周龄雄性野生型C57BL/6小鼠共6只购自湖北省实验动物中心，体重22~26 g，合格证号：SCXK（鄂）2025-0018。小鼠饲养于SPF级动物实验设施内，环境温度维持在22~26 ℃，相对湿度为40%~70%，采用12 h光/暗循环，自由摄食和饮水。纳入标准为骨骼完整、无外观发育异常，本实验所有小鼠均符合标准，无样本剔除。本实验遵循国家《实验动物管理条例》及

《实验动物福利伦理审查指南》的相关规定，并通过单位实验动物伦理委员会批准（审批号：S07925020D）。采用全骨髓贴壁法分离培养BMSCs[10]。将小鼠脱颈处死后，在无菌条件下分离股骨和胫骨；剪去骨骺端，用αMEM培养基冲洗骨髓腔，收集冲洗液。将所得细胞悬液离心重悬，接种于培养瓶中，使用完全培养基（αMEM+10%FBS+1%青霉素-链霉素），置于37 ℃、5% CO_2的培养箱内培养，48 h后首次半换液，72 h后全换液。在细胞融合度达到80%~90%时进行传代培养，用于后续实验。流式细胞术检测表面标志物CD29、CD90.2、CD11b和CD45的表达量。

1.2.2　依托泊苷诱导BMSCs衰老模型的建立及最适浓度筛选　将BMSCs分为5组：0、5、10、15、20 μmol/L依托泊苷处理组，处理细胞48 h后更换新鲜完全培养基，继续培养48 h。CCK-8检测细胞活力：将BMSCs以3×10³细胞/孔的密度接种于96孔板，细胞贴壁后，分别加入0、5、10、15、20 μmol/L依托泊苷，加入CCK-8试剂孵育2 h，酶标仪测量吸光度（450 nm）。

qRT-PCR检测衰老相关mRNA表达：使用Trizol试剂从细胞中提取总RNA，使用HiScript II Q RT SuperMix for qPCR试剂将RNA逆转录为cDNA，采用SYBR Green染料法进行定量分析，用$2^{-\Delta\Delta Ct}$法测定基因相对表达水平。检测p53、p21、p16 mRNA表达。引物序列见表1。

表1　qRT-PCR引物序列

Table 1　Primer sequences used for qRT-PCR

Genes	Forward primers（5'→3'）	Reverse primers（3'→5'）
p53	GTCACAGCACATGACGGAGG	TCTTCCAGATGCTCGGGATAC
p21	ATGTCCAATCCTGGTGATGTC	GAAGTCAAAGTTCCACCGTTC
p16	TCAAGACATCGTGCGATATTTG	TTAGCTCTGCTCTTGGGATTG
Ldha	TCCGTTACCTGATGGGAGAG	GCAACATTCACACCACTCCA
Ep300	GAAGAACAGCCAAGCACCACCTC	CGGTAAAGTGCCCCCAATGT
Sirt2	CAGCTACTTCAAGAAACATCCG	TATTCTTTTCTGCAGGAGGTGT
Runx2	AACGATCTGAGATTTGTGGGC	CCTGCGTGGGATTTCTTGGTT
Sp7	GGCTTTTCTGCGGCAAGAGGTT	CGCTGATGTTTGCTCAAGTGGTC
Alpl	CCAACTCTTTTGTGCCAGAGA	GGCTACATTGGTGTTGAGCTTTT
Gapdh	GTGGCAAAGTGGAGATTGTTG	CGTTGAATTTGCCGTGAGTG

p53: Tumor protein p53; p21: Cyclin-dependent kinase inhibitor 1A; p16: Cyclin-dependent kinase inhibitor 2A; Ldha: Lactate dehydrogenase A; Ep300: E1A binding protein p300; Sirt2: Sirtuin 2; Runx2: Runt-related transcription factor 2; Sp7: Sp7 transcription factor; Alpl: Alkaline phosphatase; Gapdh: Glyceraldehyde-3-phosphate dehydrogenase

Western blot检测衰老相关蛋白表达：收集细胞，裂解后超声破碎，离心取上清液，使用BCA蛋白浓度测定试剂盒对样品进行定量。将蛋白样品经SDS-聚丙烯酰胺凝胶电泳分离后，转至聚偏二氟乙烯膜上。膜在室温下使用5%脱脂奶粉封闭1 h后，于4 ℃孵育目标一抗过夜，第二天用相应二抗室温孵育1 h。用ECL发光试剂盒进行检测。蛋白条带通过凝胶成像系统显影，用ImageJ软件进行灰度分析。检测P53、P21、P16蛋白表达。

SA-β-gal染色：使用0、10 μmol/L依托泊苷处理BMSCs，48 h后更换新鲜完全培养基，继续培养48 h后，采用β-半乳糖苷酶染色试剂盒，按照制造商说明检测细胞衰老[11]。细胞经PBS洗涤后，于室温固定15 min。随后，按说明书配制染色工作液，对细胞进行染色并在37 ℃过夜孵育。通过倒置显微镜观察并分析细胞的染色情况。

根据以上结果确定依托泊苷的最适诱导浓度（10 μmol/L）。

1.2.3　衰老BMSCs乳酸生成及组蛋白乳酸化水平检测　采用随机数字表法将BMSCs培养孔分配至对照组和衰老组。衰老组使用含10 μmol/L依托泊苷的完全培养基培养；对照组使用含等体积DMSO的完全培养基培养。48 h后弃去两组细胞培养基，用PBS轻柔清洗细胞，更换为新鲜完全培养基继续培养48 h。

乳酸含量检测：收集细胞培养上清，使用乳酸检测试剂盒检测乳酸生成水平。按照制造商说明准备空白管、样品管和标准管，加入酶工作液和显色剂在37 ℃反应10 min，最后加入终止液，酶标仪测量吸光度（530 nm）。

qRT-PCR：提取细胞总RNA，检测Ldha、Ep300、Sirt2 mRNA表达（引物见表1）。

Western blot：检测Pan-Kla和H3K18la蛋白水平，以β-ACTIN或H3为内参。

1.2.4　抑制乳酸生成对BMSCs衰老表型的影响　将BMSCs分为3组：衰老组（10 μmol/L依托泊苷处理）、衰老+GNE-140组（10 μmol/L依托泊苷+1 μmol/L GNE-140处理）、对照组（含等体积DMSO溶剂的普通完全培养基）。处理48 h后更换新鲜完全培养基，继续培养48 h。

检测指标：乳酸含量（方法同1.2.3）、p53/p21/p16 mRNA（qRT-PCR）、P53/P21/P16蛋白（Western blot）、SA-β-gal阳性率（染色方法同1.2.2）。

1.2.5　外源性乳酸钠对衰老BMSCs成骨分化的影响　使用2~3代的BMSCs，将BMSCs分为对照组、衰老组、衰老+5 mmol/L乳酸钠组和衰老+10 mmol/L乳酸钠组[12-13]。衰老组及乳酸钠干预组细胞采用含10 μmol/L依托泊苷的完全培养基处理48 h，随后弃去含药培养基，更换为新鲜完全培养基继续培养48 h，以诱导细胞衰老；对照组细胞采用含等体积DMSO的完全培养基培养48 h，随后更换为新鲜完全培养基继续培养48 h。

成骨分化诱导：完成上述处理后，各组细胞均更换为成骨诱导培养基（αMEM+10%FBS+1%青霉素-链霉素+50 μg/mL维生素C+10 mmol/L β-甘油磷酸钠+100 nmol/L地塞米松）进行成骨分化诱导。衰老+5 mmol/L乳酸钠组和衰老+10 mmol/L乳酸钠组分别使用含5 mmol/L或10 mmol/L L-乳酸钠的成骨诱导培养基；对照组和衰老组使用不含乳酸钠的成骨诱导培养基，并加入与乳酸钠干预组等体积的PBS作为溶剂对照。成骨诱导期间每3 d进行半量换液，乳酸钠干预组在每次换液时均维持相同浓度的L-乳酸钠，对照组和衰老组则维持等体积溶剂对照。

检测时间点及指标：成骨诱导7 d：qRT-PCR检测Runx2、Sp7、Alpl mRNA表达（引物见表1）。成骨诱导14 d：Western blot检测COL1、RUNX2、OSX、OCN蛋白表达。成骨诱导21 d：茜素红染色观察矿化结节形成能力。茜素红染色：弃培养基，PBS洗涤，4%多聚甲醛固定15 min，PBS洗涤后加入茜素红染液，室温孵育30 min，去离子水洗净，显微镜观察拍照。

1.3　统计学分析

使用GraphPad Prism10软件进行统计学分析。采用Shapiro-Wilk检验对数据进行正态性检验，符合正态分布的计量资料以均值±标准差（$\bar{x}\pm s$）表示，所有体外实验均独立重复3次。两组间比较采用独立样本t检验，多组比较使用单因素方差分析（one-way ANOVA），组间两两比较使用Tukey多重比较检验。$P<0.05$为差异有统计学意义。

2　结　果

2.1　构建依托泊苷诱导的小鼠BMSCs衰老的细胞模型

流式细胞术鉴定显示，提取的BMSCs高表达CD29（97.3%）和CD90（95.7%），低表达CD11b（2.57%）和CD45（1.67%），符合BMSCs特征（图1）。

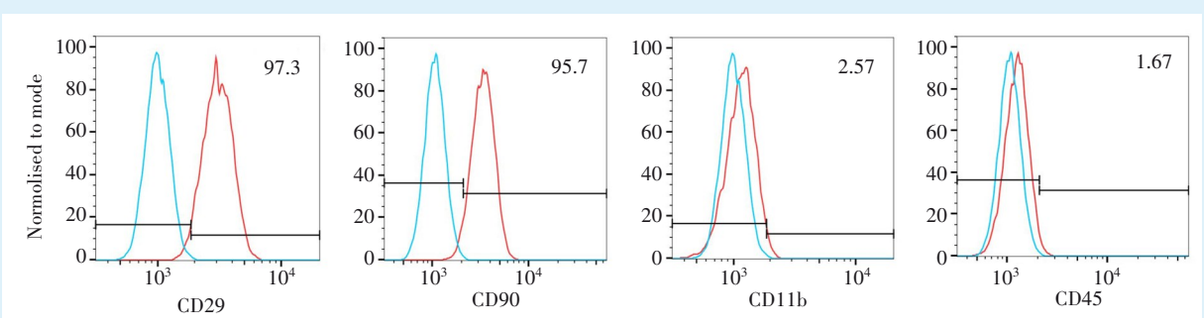

The expression of surface markers in cultured mouse BMSCs was analyzed by flow cytometry. The cells were positive for mesenchymal stem cell markers CD29 (97.3%) and CD90 (95.7%), and negative for hematopoietic markers CD11b (2.57%) and CD45 (1.67%), thus confirming the mesenchymal stem cell phenotype of the isolated cells. BMSCs: bone marrow mesenchymal stem cells; CD29: cluster of differentiation 29 (integrin beta-1); CD90: cluster of differentiation 90 (Thy-1 cell surface antigen); CD11b: cluster of differentiation 11b (Integrin alpha M); CD45: cluster of differentiation 45 (protein tyrosine phosphatase receptor type C)

Figure 1　Flow cytometric identification of mouse BMSCs

图1　小鼠BMSCs的流式细胞术鉴定

随依托泊苷浓度（0、5、10、15、20 μmol/L）增加，p53和p21的mRNA及蛋白水平逐渐升高（浓度≥10 μmol/L时与对照组比较，$P<0.05$），p16无明显变化（图2a~2c），提示依托泊苷通过激活p53-p21信号通路诱导细胞衰老。

CCK-8显示BMSCs细胞活力随浓度升高而下降，15 μmol/L时活力下降超过30%，后续选用10 μmol/L的依托泊苷浓度进行诱导（图2d）。10 μmol/L依托泊苷处理后，SA-β-gal阳性细胞比例增加（$P< 0.001$）（图2e、2f）。

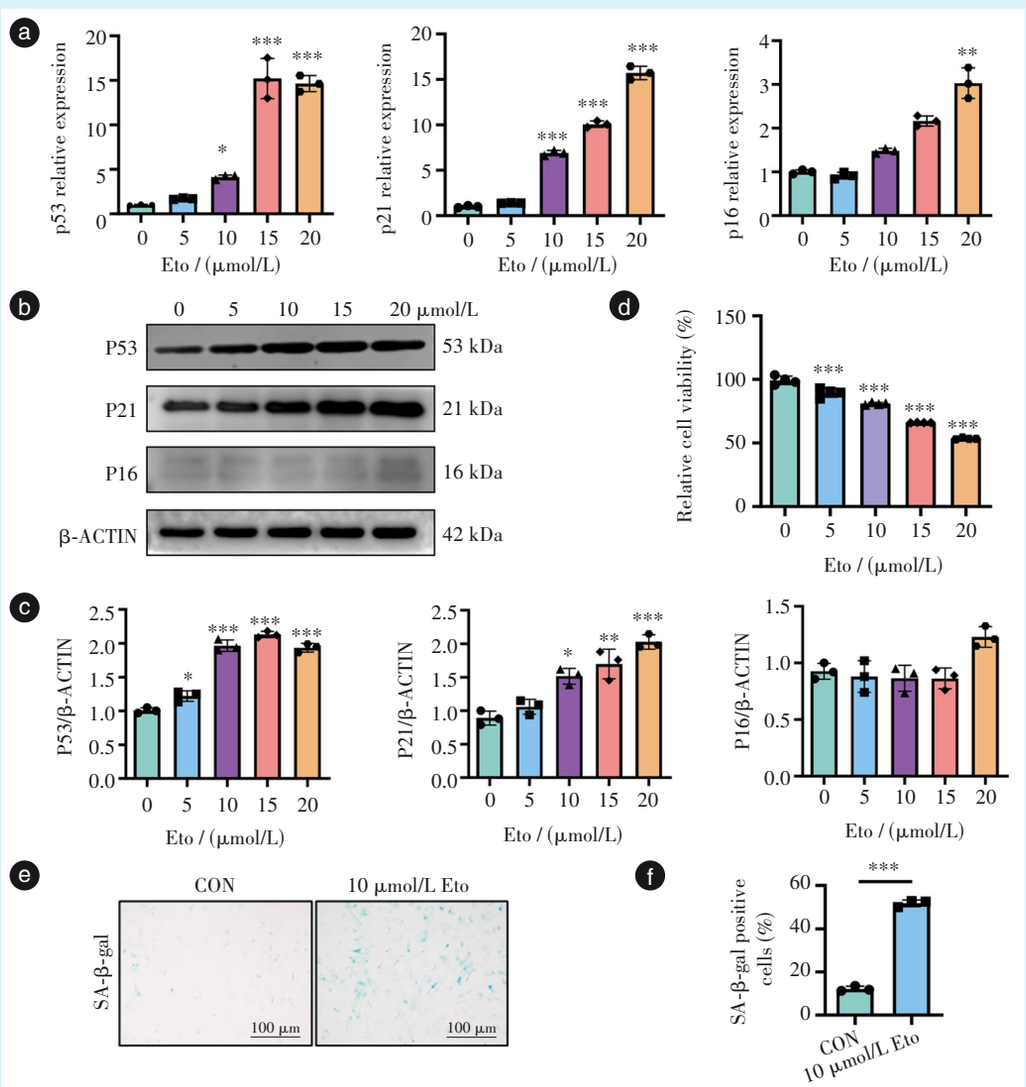

a: relative mRNA expression levels of p53, p21, and p16 in BMSCs treated with different concentrations of etoposide. The mRNA expression levels of p53 and p21 increased in a dose-dependent manner following etoposide treatment (n = 3). b: representative Western blot images showing the protein expression levels of P53, P21, and P16 in BMSCs treated with different concentrations of etoposide. c: quantitative analysis of P53, P21, and P16 protein levels normalized to β-ACTIN (n = 3). The protein levels of P53 and P21 increased in a dose-dependent manner following etoposide treatment. d: relative cell viability of BMSCs treated with different concentrations of etoposide, as determined by CCK-8 assay (n = 3). e: representative SA-β-gal images of BMSCs treated with 0 or 10 μmol/L etoposide. Treatment with 10 μmol/L etoposide significantly induced senescence in BMSCs. f: quantitative analysis of percent of SA-β-gal-positive cells of BMSCs treated with 0 or 10 μmol/L etoposide (n = 3). BMSCs: bone marrow mesenchymal stem cells; Eto: etoposide; CON: control; P53: tumor protein p53; P21: cyclin-dependent kinase inhibitor 1A; P16: cyclin-dependent kinase inhibitor 2A; β-ACTIN: beta-actin; SA-β-gal: senescence-associated β-galactosidase. Comparisons between two groups were performed using the independent samples t-test. For comparisons among multiple groups, one-way analysis of variance (ANOVA) was applied, followed by Tukey's multiple comparison test for pairwise post hoc analysis. *P<0.05, **P<0.01, ***P<0.001: compared to the CON group. The above experiments were repeated 3 times independently

Figure 2　Establishment of an etoposide-induced cellular senescence model in mouse BMSCs

图2　构建依托泊苷诱导的小鼠BMSCs衰老的细胞模型

2.2　BMSCs衰老后乳酸生成减少，泛乳酸化和组蛋白乳酸化水平下降

随依托泊苷浓度升高，BMSCs胞外乳酸水平逐渐降低（图3a）。10 μmol/L依托泊苷处理后，Ldha、Ep300的mRNA表达下降（P<0.001），而Sirt2的mRNA上调（P<0.01）（图3b）。Western blot显示，衰老BMSCs中Pan-Kla和H3K18la水平均显著下调（P<0.001），其中H3K18la约下降50%（图3c-3e）。

2.3　乳酸生成障碍加重BMSCs衰老表型

GNE-140处理使BMSCs胞外乳酸水平进一步降低（图4a）。与和对照组相比，衰老组中p53和p21的mRNA和蛋白表达水平升高（P<0.001）；而在衰老+GNE-140组中，p53和p21的mRNA和蛋白表

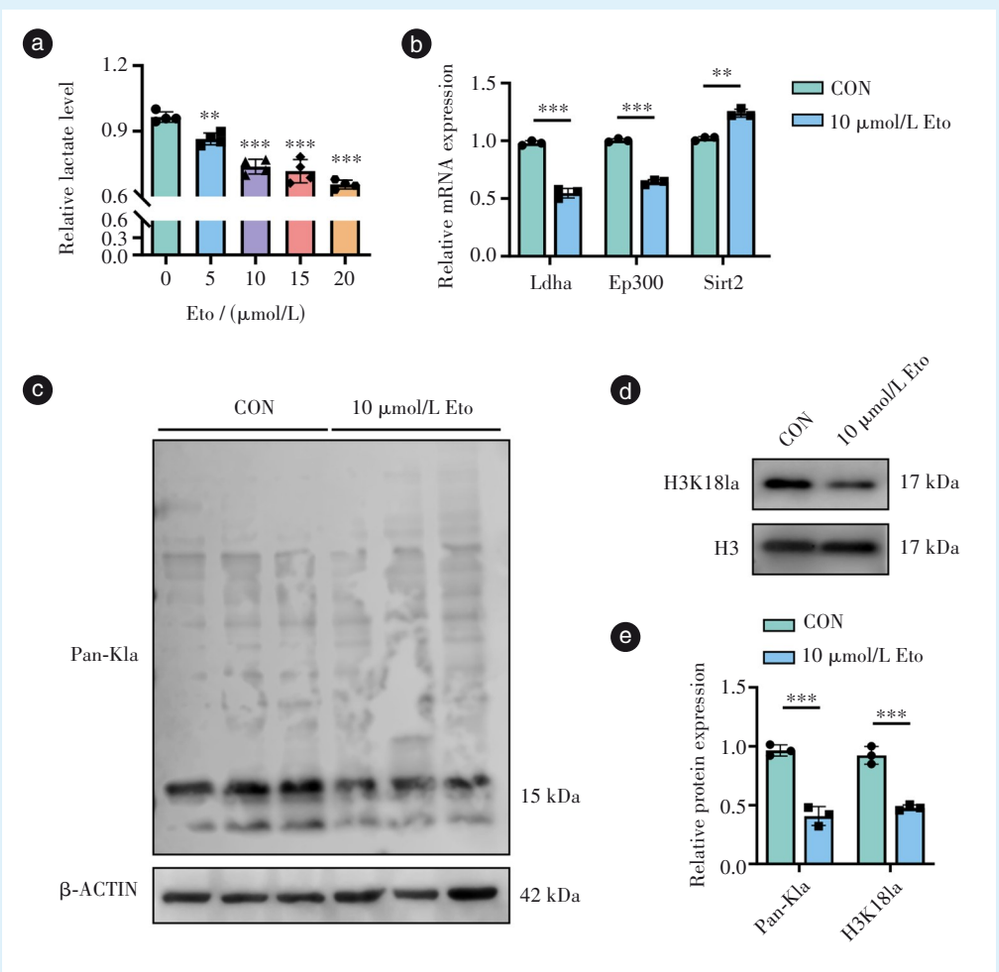

a: relative lactate levels of BMSCs treated with different concentrations of etoposide; the lactate level decreased in a dose-dependent manner following etoposide treatment (n = 3). b: relative mRNA expression levels of Ldha, Ep300, and Sirt2 in BMSCs from the CON and 10 μmol/L Eto groups. The mRNA expression levels of Ldha and Ep300 were lower in the 10 μmol/L Eto group, while mRNA expression level of Sirt2 was higher in the 10 μmol/L Eto group (n = 3). c: representative Western blot images showing protein expression levels of Pan-Kla in BMSCs from the CON and 10 μmol/L Eto groups. d: representative Western blot images showing protein expression levels of H3K18la in BMSCs from the CON and 10 μmol/L Eto groups. e: quantitative analysis of Pan-Kla and H3K18la protein levels normalized to β-ACTIN or H3, and the protein levels of Pan-Kla and H3K18la were decreased in the 10 μmol/L Eto group (n = 3) (P<0.001). BMSCs: bone marrow mesenchymal stem cells; Eto: etoposide; CON: control; Ldha: lactate dehydrogenase A; Ep300: E1A binding protein P300; Sirt2: sirtuin 2; Pan-Kla: pan-lysine lactylation; β-ACTIN: beta-actin; H3K18la: histone H3 lysine 18 lactylation; H3.: histone H3. Comparisons between two groups were performed using the independent samples t-test. For comparisons among multiple groups, one-way analysis of variance (ANOVA) was applied, followed by Tukey's multiple comparison test for pairwise post hoc analysis. **P<0.01, ***P<0.001: compared to the CON group. The above experiments were repeated 3 times independently

Figure 3　Senescent BMSCs exhibit reduced lactate production and decreased levels of pan-lactic acid and histone lactylation

图3　BMSCs衰老后乳酸生成减少，泛乳酸化和组蛋白乳酸化水平下降

达水平进一步升高(P<0.001)(图4b-4d)。

SA-β-gal染色结果也显示,衰老+GNE-140组中衰老阳性细胞最多(图4e、4f)。

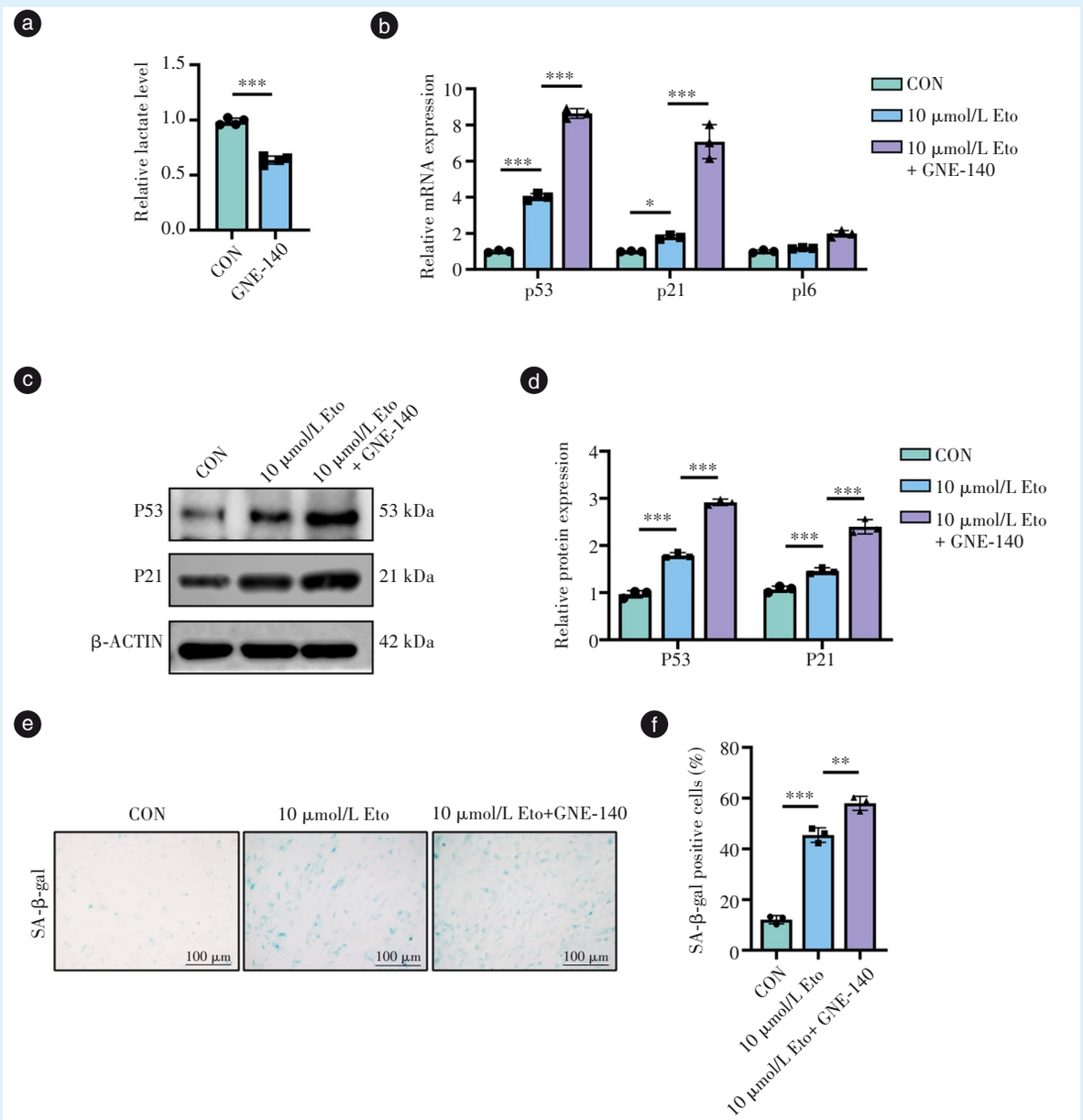

a: relative lactate levels of BMSCs treated with nothing or GNE-140; the lactate level decreased following GNE-140 treatment (n = 3). b: relative mRNA expression levels of p53, p21, and p16 in BMSCs. The mRNA expression levels of p53 and p21 were highest in the 10 μmol/L Eto+ GNE-140 group (n = 3). c: representative Western blot images showing protein expression levels of P53 and P21 in BMSCs. d: quantitative analysis of P53and P21 protein levels normalized to β-ACTIN. The protein levels of P53 and P21 were highest in the 10 μmol/L Eto+ GNE-140 group (n = 3). e: representative SA-β-gal images of BMSCs. f: quantitative analysis of the percentage of SA-β-gal-positive cells showed that the 10 μmol/L Eto+ GNE-140 group exhibited the highest proportion of positive cells (n = 3). BMSCs: bone marrow mesenchymal stem cells; GNE-140: the compound code for a small-molecule inhibitor of lactate dehydrogenase; Eto: etoposide; CON: control; P53: tumor protein p53; P21: cyclin-dependent kinase inhibitor 1A; P16: cyclin-dependent kinase inhibitor 2A; β-ACTIN: beta-actin; SA-β-gal: senescence-associated β-galactosidase. Comparisons between two groups were performed using the independent samples t-test. For comparisons among multiple groups, one-way analysis of variance (ANOVA) was applied, followed by Tukey's multiple comparison test for pairwise post hoc analysis. **P<0.01, ***P<0.001: compared to the CON group. The above experiments were repeated 3 times independently

Figure 4　Inhibition of lactate production exacerbates etoposide-induced senescence in BMSCs

图4　抑制乳酸生成加重依托泊苷诱导的BMSCs衰老表型

2.4　外源性补充乳酸钠能够缓解衰老BMSCs的成骨分化障碍

5、10 mmol/L乳酸钠处理以浓度依赖性方式增加Pan-Kla和H3K18la水平（P<0.01，P<0.001），且不影响细胞活力（图5）。

衰老BMSCs中Runx2、Sp7、Alpl mRNA及COL1、RUNX2、OSX、OCN蛋白表达均显著降低（P<0.001）；补充5、10 mmol/L乳酸钠后，上述指标显著回升（P<0.05，P<0.01，P<0.001），且茜素红染色显示的矿化结节形成能力增强（图6）。

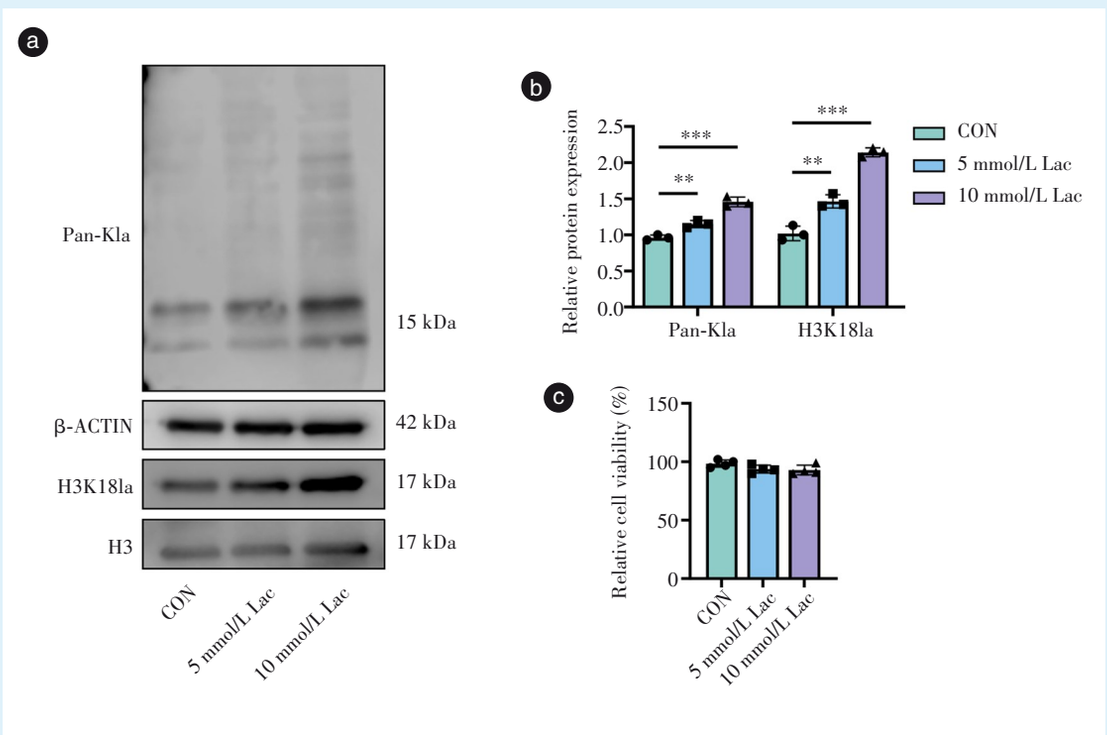

a: representative Western blot images showing the protein expression levels of Pan-Kla and H3K18la in BMSCs treated with 0, 5 mmol/L Lac, and 10 mmol/L Lac. b: quantitative analysis of the Pan-Kla protein level normalized to β-ACTIN and the H3K18la level normalized to H3 (n = 3). c: relative cell viability of BMSCs treated with 0, 5 mmol/L Lac, and 10 mmol/L Lac, as determined by a CCK-8 assay (n = 3). The protein levels of Pan-Kla and H3K18la increased in a dose-dependent manner following sodium lactate treatment. BMSCs: bone marrow mesenchymal stem cells; CON: control; Lac: sodium lactate; Pan-Kla: pan-lysine lactylation; β-ACTIN: beta-actin; H3K18la: histone H3 lysine 18 lactylation; H3: histone H3. For comparisons among multiple groups, one-way analysis of variance (ANOVA) was applied, followed by Tukey's multiple comparison test for pairwise post hoc analysis. **P<0.01, ***P<0.001: compared to the CON group. The above experiments were repeated 3 times independently

Figure 5　Sodium lactate treatment increases both pan-lactylation and histone lactylation levels of BMSCs

图5　乳酸钠处理增加BMSCs的泛乳酸化和组蛋白乳酸化水平

3　讨　论

本研究以小鼠BMSCs衰老模型为基础，系统探讨了衰老过程中乳酸代谢及组蛋白乳酸化修饰的变化特征，并分析了调控乳酸水平对衰老BMSCs成骨分化能力的影响，为衰老相关骨再生和修复障碍的表观遗传机制提供新的视角。

3.1　BMSCs衰老与乳酸生成障碍的关系

细胞衰老常伴随代谢重编程，糖酵解能力下降和线粒体功能异常是典型特征[14-16]。糖酵解下降会减少丙酮酸和还原型烟酰胺腺嘌呤二核苷酸（reduced nicotinamide adenine dinucleotide，NADH）的生成，导致乳酸脱氢酶反应底物不足，并影响氧化型烟酰胺腺嘌呤二核苷酸（oxidized nicotinamide adenine dinucleotide，NAD^+）/NADH平衡，从而导致乳酸产生减少[17-18]。

本研究使用不同浓度的依托泊苷诱导BMSCs的衰老[19-20]，依托泊苷作为拓扑异构酶Ⅱ抑制剂可诱导DNA双链断裂并激活DNA损伤反应。既往研究表明，在DNA损伤诱导的应激性衰老中，p53-p21信号通路是主要激活的调控通路，而p16-Rb通

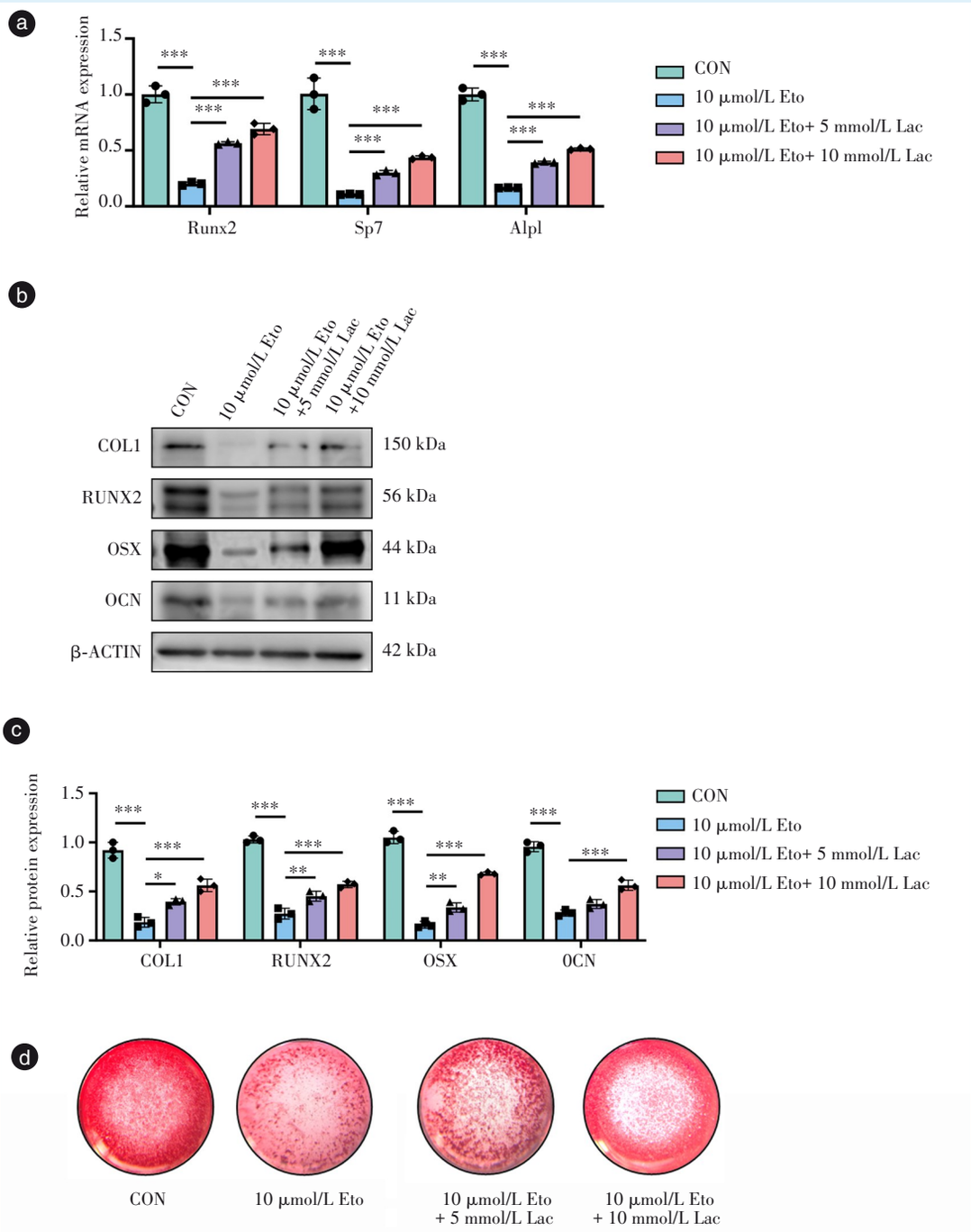

a: relative mRNA expression levels of Runx2, Sp7, and Alp1 in BMSCs. The mRNA expression levels of these osteogenic markers were significantly downregulated in the etoposide-treated group (P<0.001), and were partially restored by treatment with 5 mmol/L or 10 mmol/L sodium lactate (n = 3). b: representative Western blot images showing the protein expression levels of COL1, RUNX2, OSX, and OCN in BMSCs. c: quantitative analysis of COL1, RUNX2, OSX, and OCN protein levels normalized to β-ACTIN. The protein levels of these osteogenic markers were significantly downregulated in the etoposide-treated group (P<0.001), and were partially restored by treatment with 5 mmol/L or 10 mmol/L sodium lactate (n = 3). d: representative ARS staining images showing mineralized ability of BMSCs. BMSCs: bone marrow mesenchymal stem cells; CON: control; Eto: etoposide; Lac: sodium lactate; Runx2: runt-related transcription factor 2; Sp7/OSX: transcription factor Sp7/osterix; Alpl: alkaline phosphatase; COL1: collagen type I; OCN: osteocalcin; β-ACTIN: beta-actin; ARS: Alizarin Red S. For comparisons among multiple groups, one-way analysis of variance (ANOVA) was applied, followed by Tukey's multiple comparison test for pairwise post hoc analysis. *P<0.05, **P<0.01, ***P<0.001: compared to the CON group. The above experiments were repeated 3 times independently

Figure 6　Sodium lactate supplementation alleviates the impairment of osteogenic differentiation in senescent BMSCs

图6　外源性补充乳酸钠能够缓解衰老BMSCs的成骨分化障碍

路在不同细胞类型或诱导条件下可能不显著上调[21]。

本研究中，随着BMSCs衰老程度的加重，细胞外乳酸生成水平逐渐降低，提示BMSCs在衰老过程中存在乳酸生成障碍，这与Sun等[22]的结果一致，同样在血管衰老[23]、骨骼肌衰老[24]等过程中也存在乳酸生成的减少。但在阿尔茨海默病、慢性阻塞性肺疾病、糖尿病等和衰老相关的疾病条件下，乳酸水平可能升高并驱动细胞和组织衰老[25-27]。进一步使用乳酸脱氢酶抑制剂GNE-140[28]抑制乳酸生成后，P53、P21表达水平及SA-β-gal阳性细胞比例进一步升高，说明乳酸代谢下降不仅是衰老的伴随现象，还可能参与衰老表型的维持或加重过程[24]。这一结果支持代谢异常在干细胞衰老发生发展中的功能性作用[29-30]。

3.2　组蛋白乳酸化修饰水平下降可能介导衰老相关转录重塑

乳酸不仅是代谢产物，还可通过乳酸化修饰参与表观遗传调控。近年来，组蛋白乳酸化被认为是一种将细胞代谢状态直接转化为基因表达调控信号的重要机制[31-33]。本研究发现，BMSCs衰老过程中泛乳酸化水平显著下降，且主要发生于组蛋白H3；同时，组蛋白乳酸化修饰标记H3K18la水平明显下调。这提示，衰老相关的乳酸代谢障碍可能通过降低组蛋白乳酸化水平，改变染色质状态及相关基因的转录活性[24]，从而影响BMSCs的功能维持和分化潜能。这一结果为理解干细胞衰老过程中代谢状态如何通过表观遗传机制影响细胞功能提供了新的证据。

3.3　乳酸-组蛋白乳酸化轴在成骨分化调控中的潜在作用

成骨分化是BMSCs维持骨稳态和骨再生能力的关键功能[34-35]。已有研究显示H3K18la能促进成骨分化[36-37]。结合前述结果推测，乳酸补充可能通过恢复细胞内乳酸水平，提高组蛋白乳酸化修饰，从而促进成骨相关基因的转录激活，部分逆转衰老导致的成骨分化障碍。这一发现为代谢-表观遗传调控成骨分化提供了新依据。

BMSCs衰老的研究多集中于氧化应激、DNA损伤或经典表观遗传修饰（如乙酰化和甲基化），而乳酸代谢及组蛋白乳酸化在BMSCs衰老中的作用尚缺乏系统研究。本研究从乳酸代谢及组蛋白乳酸化修饰的角度，揭示了衰老BMSCs成骨分化障碍可能与乳酸-组蛋白乳酸化轴失衡有关，为骨衰老中代谢与表观遗传互作机制提供了新视角。

综上所述，本研究从代谢—表观遗传互作的角度，揭示了乳酸代谢及组蛋白乳酸化在BMSCs衰老及成骨分化调控中的潜在作用，为理解衰老相关骨质疏松和骨再生障碍的分子机制提供了新的视角。然而，本研究仍存在一定局限性：仅在体外细胞模型中进行验证，尚缺乏体内水平的功能证据；组蛋白乳酸化调控的具体靶基因及其上游酶促机制（如Ldha[38]、Sirt2[39]、Ep300[7]）仍有待进一步深入研究。未来可结合动物模型及染色质层面的研究手段，进一步阐明乳酸-组蛋白乳酸化轴在骨衰老和骨再生中的精确调控机制。

【Author contributions】 Guo XF performed experiments, analyzed the data and drafted the manuscript. Nie YS performed the experiments and revised the article. Yang GB designed the study and revised the article. All authors read and approved the final manuscript as submitted.

【Ethics Statement】 This study was conducted in accordance with the national Regulations for the Administration of Laboratory Animals and the Guidelines for Ethical Review of Laboratory Animal Welfare, and approved by the Animal Ethics Committee of the institution (Approval No. S07925020D).

【Funding】 This study was supported by the grant from National Natural Science Foundation of China (No. 82270947). The funder had no role in the study design, data collection and analysis, decision to publish, or preparation of the manuscript.

【Competing interests】 All authors have completed the ICMJE uniform disclosure form at www.icmje.org/disclosure-of-interest/ and declare: support from the National Natural Science Foundation of China (No. 82270947) for the submitted work; no financial relationships with any organisations that might have an interest in the submitted work in the previous three years; no other relationships or activities that could appear to have influenced the submitted work.

【Data availability statement】 The original contributions presented in this study are included in the article. Further inquiries can be directed to the corresponding author upon reasonable request.

【Generative AI statement】 The authors declared that generative AI was not used in the creation of this manuscript.

参考文献

[1] Chen Q, Shou P, Zheng C, et al. Fate decision of mesenchymal stem cells: adipocytes or osteoblasts?[J]. Cell Death Differ, 2016, 23(7): 1128-1139. doi: 10.1038/cdd.2015.168.

[2] Sun D, Chen Y, Liu X, et al. miR-34a-5p facilitates osteogenic differentiation of bone marrow mesenchymal stem cells and modulates bone metabolism by targeting HDAC1 and promoting ER-α transcription[J]. Connect Tissue Res, 2023, 64(2): 126-138. doi: 10.1080/03008207.2022.2108415.

[3] Zhao Y, He J, Qiu T, et al. Epigenetic therapy targeting bone marrow mesenchymal stem cells for age-related bone diseases[J]. Stem Cell Res Ther, 2022, 13(1): 201. doi: 10.1186/s13287-022-

02852-w.

[4] Hu L, Yin C, Zhao F, et al. Mesenchymal stem cells: cell fate decision to osteoblast or adipocyte and application in osteoporosis treatment[J]. Int J Mol Sci, 2018, 19(2): 360. doi: 10.3390/ijms19020360.

[5] Yang S, Ma Y, Wu T, et al. Lactate transmission from hypoxic tumor cells promotes macrophage senescence and M2 polarization *via* the DNMT1-NHE7 axis to accelerate endometrial cancer progression[J]. Cell Death Dis, 2026, 17(1): 185. doi: 10.1038/s41419-026-08411-y.

[6] Zhao X, Lin Y, Lin P, et al. Decoding dental stem cell aging: mechanisms, therapeutic strategies, and beyond[J]. Adv Sci, 2025, 12(44): e04969. doi: 10.1002/advs.202504969.

[7] Huang J, Wang X, Li N, et al. YY1 lactylation aggravates autoimmune uveitis by enhancing microglial functions *via* inflammatory genes[J]. Adv Sci, 2024, 11(19): e2308031. doi: 10.1002/advs.202308031.

[8] Xu W, Zhao A, Han R, et al. Extracellular lactate improves neurogenesis by modulating H3K9 lactylation and SnoN expression under hypoxic conditions[J]. Stem Cell Res Ther, 2025, 16(1): 462. doi: 10.1186/s13287-025-04571-4.

[9] Zeng M, Liu H, Lu W, et al. Lactate-functionalized 3D-printed PCL/nHA scaffold drives BMSC osteogenesis *via* metabolic-epigenetic crosstalk[J]. Mater Today Bio, 2025, 33: 102101. doi: 10.1016/j.mtbio.2025.102101.

[10] 丁梦, 李强, 李筱叶, 等. 光固化水凝胶负载骨髓间充质干细胞修复大鼠颅骨缺损[J]. 口腔疾病防治, 2024, 32(5): 330-340. doi: 10.12016/j.issn.2096-1456.2024.05.002.
Ding M, Li Q, Li XY, et al. Reconstruction of rat calvarial defects utilizing an ultraviolet-cured hydrogel loaded with bone marrow mesenchymal stem cells[J]. J Prev Treat Stomatol Dis, 2024, 32(5): 330-340. doi: 10.12016/j.issn.2096-1456.2024.05.002.

[11] Lee BY, Han JA, Im JS, et al. Senescence-associated β-galactosidase is lysosomal β-galactosidase[J]. Aging Cell, 2006, 5(2): 187-195. doi: 10.1111/j.1474-9726.2006.00199.x.

[12] Meng M, Zhao X, Zheng X, et al. Lactate inhibits mouse embryonic palatal mesenchyme cells chondrogenesis through AKT-PKM2 axis[J]. BMC Oral Health, 2025, 25(1): 1289. doi: 10.1186/s12903-025-06632-9.

[13] Guo Y, He L, Xue A, et al. Exercise increases bone mass by lactate/Gpr81 signaling pathway[J]. Commun Biol, 2025, 8(1): 1548. doi: 10.1038/s42003-025-08957-1.

[14] Wu Y, Tang L, Huang H, et al. Phosphoglycerate dehydrogenase activates PKM2 to phosphorylate histone H3T11 and attenuate cellular senescence[J]. Nat Commun, 2023, 14(1): 1323. doi: 10.1038/s41467-023-37094-8.

[15] Ramírez-Pardo I, Campanario S, Chavda B, et al. Chaperone-mediated autophagy sustains muscle stem cell regenerative functions but declines with age[J]. Nat Metab, 2025, 7(12): 2571-2588. doi: 10.1038/s42255-025-01411-w.

[16] Miwa S, Kashyap S, Chini E, et al. Mitochondrial dysfunction in cell senescence and aging[J]. J Clin Invest, 2022, 132(13): e158447. doi: 10.1172/JCI158447.

[17] Robergs RA, McNulty CR, Minett GM, et al. Lactate, not lactic acid, is produced by cellular cytosolic energy catabolism[J]. Physiology, 2018, 33(1): 10-12. doi: 10.1152/physiol.00033.2017.

[18] Cerdán S, Rodrigues TB, Sierra A, et al. The redox switch/redox coupling hypothesis[J]. Neurochem Int, 2006, 48(6/7): 523-530. doi: 10.1016/j.neuint.2005.12.036.

[19] Zhou Z, Kang K, Wang H, et al. H3K27 acetylation-driven IGF2BP2 mutates during the aging of MSCs, thereby influencing osteogenic differentiation and bone aging[J]. Int J Biol Sci, 2026, 22(1): 142-160. doi: 10.7150/ijbs.122708.

[20] Hu M, Xing L, Zhang L, et al. NAP1L2 drives mesenchymal stem cell senescence and suppresses osteogenic differentiation[J]. Aging Cell, 2022, 21(2): e13551. doi: 10.1111/acel.13551.

[21] Yosef R, Pilpel N, Papismadov N, et al. p21 maintains senescent cell viability under persistent DNA damage response by restraining JNK and caspase signaling[J]. EMBO J, 2017, 36(15): 2280-2295. doi: 10.15252/embj.201695553.

[22] Sun Y, Yu X, Gao X, et al. RNA sequencing profiles reveal dynamic signaling and glucose metabolic features during bone marrow mesenchymal stem cell senescence[J]. Cell Biosci, 2022, 12(1): 62. doi: 10.1186/s13578-022-00796-5.

[23] Wang Y, Chen J, Wang X, et al. TRPM7 deficiency accelerates vascular senescence by inhibiting H3K18 lactylation[J]. Aging Cell, 2025, 24(11): e70244. doi: 10.1111/acel.70244.

[24] Meng F, He J, Zhang X, et al. Histone lactylation antagonizes senescence and skeletal muscle aging by modulating aging-related pathways[J]. Adv Sci, 2025, 12(22): e2412747. doi: 10.1002/advs.202412747.

[25] Wei L, Yang X, Wang J, et al. H3K18 lactylation of senescent microglia potentiates brain aging and Alzheimer's disease through the NFκB signaling pathway[J]. J Neuroinflammation, 2023, 20(1): 208. doi: 10.1186/s12974-023-02879-7.

[26] Yang C, Wang Q, Xiong Y, et al. Histone H4 lysine 12 lactylation promotes the senescence of alveolar epithelial type II cells in chronic obstructive pulmonary disease by modulating the CD38-NAD^+ signaling pathway[J]. Aging Dis, 2025. doi: 10.14336/AD.2025.0291.

[27] Ge X, Wang S, Li Z, et al. Lactate-activated GPR132-Src signal induces macrophage senescence and aggravates atherosclerosis under diabetes[J]. Adv Sci, 2025, 12(33): e00141. doi: 10.1002/advs.202500141.

[28] Zhao SS, Liu J, Wu QC, et al. Lactate regulates pathological cardiac hypertrophy *via* histone lactylation modification[J]. J Cell Mol Med, 2024, 28(16): e70022. doi: 10.1111/jcmm.70022.

[29] Karim M, Yaku K, Kim JD, et al. Early-life NAD^+ deficiency programs skeletal muscle aging by sustained suppression of hyaluronic acid synthesis beginning in childhood[J]. Cell Rep, 2026, 45(2): 116912. doi: 10.1016/j.celrep.2025.116912.

[30] Morris S, Marx N, Barrientos G, et al. Disruption of ATP synthase spatiotemporal organization, Ca^{2+} dynamics, and contractile function in senescent cardiomyocytes[J]. Aging Cell, 2026, 25(2): e70388. doi: 10.1111/acel.70388.

[31] Zhang Y, Wang J, Li C, et al. Protein lactylation in cancer and

other pathologies: epigenetic regulation of glycolysis and its therapeutic perspectives[J]. Semin Cancer Biol, 2026, 118: 28-43. doi: 10.1016/j.semcancer.2025.12.005.

[32] Liu L, Zhang J, Dong Z, et al. Histone lactylation-mediated metabolic remodeling in vascular smooth muscle cells aggravates aortic aneurysm and dissection by promoting lactate accumulation[J]. Circulation, 2026, 153(3): 189-209. doi: 10.1161/CIRCULATIONAHA.125.072576.

[33] Wu G, Chen M, Li C, et al. Histone lactylation couples FSH-driven lactate metabolism to mitochondrial biogenesis by enhancing HDAC4-mediated deacetylation of PGC-1α in granulosa cells [J]. Research, 2026, 9: 1045. doi: 10.34133/research.1045.

[34] Arthur A, Gronthos S. Clinical application of bone marrow mesenchymal stem/stromal cells to repair skeletal tissue[J]. Int J Mol Sci, 2020, 21(24): 9759. doi: 10.3390/ijms21249759.

[35] Miteva M, Mihaylova Z, Mitev V, et al. A review of stem cell attributes derived from the oral cavity[J]. Int Dent J, 2024, 74(5): 1129-1141. doi: 10.1016/j.identj.2024.03.008.

[36] Chen H, Hua C, Chang SJ, et al. H3K18 lactylation-hexokinase 2 positive feedback loop promotes osteogenesis of ASPCs in facial infiltrating lipomatosis[J]. Stem Cell Res Ther, 2025, 16(1): 538. doi: 10.1186/s13287-025-04651-5.

[37] Wu J, Hu M, Jiang H, et al. Endothelial cell-derived lactate triggers bone mesenchymal stem cell histone lactylation to attenuate osteoporosis[J]. Adv Sci, 2023, 10(31): e2301300. doi: 10.1002/advs.202301300.

[38] Li X, Gong H, Xiong C, et al. LDHA induces beta cell dedifferentiation in diabetes through metabolic and epigenetic reprogramming[J]. Diabetologia, 2026, 69(3): 689-709. doi: 10.1007/s00125-025-06626-w.

[39] Sun L, Zhang Y, Yang B, et al. Lactylation of METTL16 promotes cuproptosis *via* m^{6}A-modification on FDX1 mRNA in gastric cancer[J]. Nat Commun, 2023, 14(1): 6523. doi: 10.1038/s41467-023-42025-8.

（编辑　罗燕鸿，于光涛）

Open Access
This article is licensed under a Creative Commons Attribution 4.0 International License.
Copyright © 2026 by Editorial Department of Journal of Prevention and Treatment for Stomatological Diseases

官网